Published in final edited form as:
Nat Struct Mol Biol. ; 18(10): 1102–1108. doi:10.1038/nsmb.2120.

Correlated structural kinetics and retarded solvent dynamics at the metalloprotease active site

Moran Grossman[1,2,6], **Benjamin Born**[3,6], **Matthias Heyden**[3,6], **Dmitry Tworowski**[1], **Gregg B Fields**[4,5], **Irit Sagi**[1,2,6], and **Martina Havenith**[3,6]

[1]Department of Structural Biology, The Weizmann Institute of Science, Rehovot, Israel.

[2]Department of Biological Regulation, The Weizmann Institute of Science, Rehovot, Israel.

[3]Lehrstuhl für Physikalische Chemie II, Ruhr-Universität Bochum, Bochum, Germany.

[4]Department of Biochemistry, The University of Texas Health Science Center, San Antonio, Texas, USA.

[5]The Torrey Pines Institute for Molecular Studies, Port St. Lucie, Florida, USA.

Abstract

Solvent dynamics can play a major role in enzyme activity, but obtaining an accurate, quantitative picture of solvent activity during catalysis is quite challenging. Here, we combine terahertz spectroscopy and X-ray absorption analyses to measure changes in the coupled water-protein motions during peptide hydrolysis by a zinc-dependent human metalloprotease. These changes were tightly correlated with rearrangements at the active site during the formation of productive enzyme-substrate intermediates and were different from those in an enzyme–inhibitor complex. Molecular dynamics simulations showed a steep gradient of fast-to-slow coupled protein-water motions around the protein, active site and substrate. Our results show that water retardation occurs before formation of the functional Michaelis complex. We propose that the observed gradient of coupled protein-water motions may assist enzyme-substrate interactions through water-polarizing mechanisms that are remotely mediated by the catalytic metal ion and the enzyme active site.

Efficient enzyme catalysis is thought to be attributable mainly to direct structural interaction between the enzyme and the substrate through the ‘lock-and-key’ or the ‘induced fit’ mechanisms[1]. Although static structures are known to have many enzymes, it is now becoming widely accepted that the functions of these enzymes are mediated by their dynamic character and by interactions with the solvent. Emerging experimental and theoretical approaches have outlined the current view, in which protein motions and conformational changes with a wide range of timescales dominate enzymatic reaction-rate enhancements[2–12]. The role of protein functional dynamics is associated with overall

Correspondence should be addressed to I.S. (irit.sagi@weizmann.ac.il) and M. Ha. (martina.havenith@rub.de)..
[6]These authors contributed equally to this work.

AUTHOR CONTRIBUTIONS

I.S. and M.Ha. are equal contributors and designed the experiments, analyzed the data and wrote the manuscript. M.G., B.B. and M.He. are equal contributors and conducted the research, analyzed the data and wrote the manuscript. D.T. constructed the enzyme-substrate docking model. G.B.F. provided the substrates.

Note: Supplementary information is available on the Nature Structural & *Molecular Biology website.*

COMPETING FINANCIAL INTERESTS

The authors declare no competing financial interests.

structural organization of the protein scaffold before catalysis. However, whether fast protein motions in time scales on the order of femtoseconds to picoseconds are linked to the chemistry of the enzymatic reaction is still under debate[12–15]. Notably, models describing protein dynamics during enzymatic reactions rarely account for the individual contribution of solvent dynamics to enzyme catalysis, despite its evident importance in controlling functional motion of proteins[16–19]. So far, water molecules at protein-water interfaces (hydration water or 'interfacial water') have been shown to thermodynamically stabilize the native structure of biomacromolecules[20], affect protein flexibility and shape the free-energy folding funnel that drives protein folding[21]. The choice of solvent has been shown to be crucial for enzyme catalysis[22]. Computational studies point out the importance of water dynamics for protein folding and function[23–28]. However, experimental information on the molecular details linking solvent dynamics and protein functional motion with enzymatic turnover is scant[29–31]. Thus, it is part of an ongoing discussion whether the contribution of solvent dynamics to protein functional motions might be essential to understand substrate binding and to improve rational drug design.

Here, we set out to experimentally quantify the real-time interplay between enzyme function and water motions during the ubiquitous enzymatic reaction of peptide hydrolysis by a metalloprotease. We merged time-resolved spectroscopic techniques, including transient fluorescence kinetics and stopped-flow X-ray absorption spectroscopy (XAS)[32,33], with kinetic terahertz absorption (KITA) spectroscopy[34]. This enabled us to simultaneously follow local active site structural-kinetic rearrangements on an atomic scale as well as global collective protein-solvent motions, both with a time resolution of milliseconds (**Fig. 1**). Accompanying molecular dynamics simulations provided a microscopic picture of the changes in the coupled water-protein motions associated with substrate binding. Overall, our results show correlated kinetics for active site structural rearrangement and water dynamics during execution of the catalytic function.

RESULTS

Identification of kinetic phases during metalloprotease turnover

The catalytic domain of human membrane type-1 matrix metalloproteinase (MT1-MMP) was used as a model enzyme in this study (see Methods). This enzyme belongs to a broad family of zinc-dependent endopeptidases that mediate peptide hydrolysis reactions of extracellular matrix proteins under both physiological and pathological conditions[35]. Substrate hydrolysis is facilitated by a nucleophilic attack of the zinc-coordinated water molecule on the carbonyl group of the peptide bond. To determine the kinetic phases of the catalytic reaction and their lifetimes, we conducted pre–steady-state kinetic analyses of the catalytic domain of MT1-MMP during hydrolysis of a fluorogenic peptide substrate that spans the cleavage site of this enzyme (Mca-Lys-Pro-Leu-Gly-Leu-Lys(Dnp)-Ala-Arg-NH_2)[36], where Mca is 7-methoxycoumarin-4-acetyl and Dnp is 2,4-dinitrophenol (**Fig. 2** and Methods). We characterized peptide hydrolysis under conditions with a surplus of substrate such that the diffusion time of substrate molecules to the enzyme active site could be neglected. We rapidly mixed the fluorogenic peptide substrate and MT1-MMP in a stopped-flow apparatus and recorded the change in fluorescence intensity, which served as an indicator of peptide hydrolysis (**Fig. 2a**). The catalytic cycle consisted of a lag phase of 60 ms followed by a burst in fluorescence associated with peptide hydrolysis. Previously, a similar sequence of transient kinetic traces was detected using an analogous system of enzyme and substrate, which indicated productive peptide binding during the lag phase and peptide substrate cleavage by the metalloprotease[33]. We therefore attributed the kinetic lag phase that we measured (**Fig. 2a**) to the formation of a Michaelis complex between the enzyme and substrate. Overall, this real-time spectroscopic analysis provided the time frames of

individual enzyme-substrate reaction events that we further probed by stopped-flow X-ray analysis.

Correlation of turnover kinetics with hydration dynamics

To follow coupled protein-water dynamics in distinct reaction phases during peptide hydrolysis by MT1-MMP, we combined the transient kinetic analysis with state-of-the-art kinetic terahertz (THz) absorption measurements. THz absorption spectroscopy is a sensitive experimental tool to probe picosecond solvent dynamics[37,38]. In a previous *ab initio* molecular dynamics simulations study on pure water, we demonstrated that infrared (near- and mid-infrared) and THz spectra are dominated by distinctly different molecular mechanisms[39]. Although infrared spectroscopy is sensitive to localized vibrational motions and dipolar coupling of neighboring molecules, excitations at THz frequencies directly probe collective vibrational motions of the entire hydrogen bond network. These collective vibrational modes involve water molecules, which can be spatially separated by more than 5 Å. Water molecules in close proximity to biomolecular solutes (hydration water) show distinct, retarded, hydrogen bond dynamics. Changes in the coupled protein-water dynamics extending over three or four hydration shells can be sensitively detected by precise measurements of THz absorption coefficients[38,40–42]. Dynamical processes in water, such as the breaking and forming of hydrogen bonds by rotational, vibrational and translational motions, take place on picosecond time scales. Collective water motions extending over more than two hydration shells contribute to the THz spectrum between 0 and 10 THz (~300 cm^{-1})[43].

KITA experiments can be used to detect changes in coupled protein-water dynamics in real time during biological reactions[34]. We set up a THz time-domain spectrometer combined with a rapid stopped-flow mixer (**Fig. 1c** and Methods). The time resolution of this experiment was set by the mixing device at 1 ms with a dead time of 50 ms. We probed the time-dependent changes in THz absorption during enzymatic turnover by short (picoseconds), repetitive (92 MHz) THz pulses that spanned the frequency range from 0.1 to 1 THz (**Fig. 2b**). Each millisecond time point in this experiment represents an equilibrium state reached by the protein-water hydrogen bond network at the picosecond time scale. We mixed enzyme and substrate at identical ratios as in the time-resolved fluorescence experiment (**Fig. 2a**), thus allowing direct correlation between the changes in THz absorption and the distinct kinetic phases during the enzymatic reaction. We recorded the amplitude of the electric field of the THz pulse (E_{THz}) at a fixed delay time, but as a function of 'kinetic time', after the stopped-flow mixing. For each data point, we averaged approximately 10^5 pulses, corresponding to an averaging time of less than 1 ms, which was faster than the fastest kinetic event observed. The intensity at the detector is proportional to $(E_{THz})^2$. Therefore, we plotted $1 - E_{sample} \times (E_{buffer})^{-1} = (E_{buffer} - E_{sample}) \times (E_{buffer})^{-1}$, which is directly related to the change in THz absorption (**Supplementary Fig. 1**). Mixing of two buffer solutions or free enzyme with buffer (**Fig. 2b**, inset) served as control experiments. In both control experiments we found no change in THz absorption over time. However, immediately after mixing of enzyme with substrate, we observed an initial increase of THz absorption that was followed by a rapid exponential decrease of THz absorption between 50 and 64 ms after mixing (**Fig. 2b**). THz data for times much less than 50 ms are not plotted here, because the data are perturbed by turbulent mixing in the stopped-flow apparatus. The decay of THz absorption after 50 ms was found to be correlated in time with the kinetic lag phase (**Fig. 2a**), suggesting a connection between distinct enzymatic events and the changes in the entire protein-water hydrogen bond network dynamics.

Active site reorganization is associated with distinct kinetic phases

To quantify atomic level structural-kinetic events taking place during distinct catalytic phases, we used stopped-flow XAS. This technique allows the monitoring of changes in the local structure and oxidation state of the atoms in the metal ion's nearest environment (up to 5 Å) at atomic resolution and in real time during each consecutive kinetic phase[33,44]. Specifically, we quantified the changes in the local structure and total effective charge of transient zinc-protein intermediates as they evolved (i) during the initial kinetic phase of enzyme-substrate interaction (lag phase: 0–60 ms) and (ii) during peptide substrate hydrolysis (burst phase: 60–200 ms). In the free metalloprotease active site, the zinc ion is tetracoordinated to three histidine nitrogens and to one water molecule. Previously, we had shown for a different metalloprotease that the peptide substrate interacts directly with the zinc ion by forming a pentacovalent complex before hydrolysis[33].

Here, we rapidly mixed and freeze-quenched free MT1-MMP and peptide substrate in the stopped-flow freeze-quench apparatus during enzymatic turnover (see Methods). The reaction conditions were equivalent to the conditions used for the kinetic fluorescence and THz measurements, and the observations could thus be directly correlated (**Fig. 2**). We trapped sample mixtures by freezing them at times between 15 and 750 ms. Frozen samples were probed with a monochromatic X-ray beam and we collected the X-ray absorption spectra of the various time-dependent complexes at the zinc K-edge energies. We analyzed the time-dependent data according to established procedures (see **Supplementary Methods**). The spectra were Fourier transformed to provide the radial distribution of the atoms within the first and second coordination shell of the catalytic zinc ion in MT1-MMP (**Fig. 3**). We were able to detect substantial changes in the radial distribution spectra that were clearly above the noise level, indicating that the local environment of the catalytic zinc ion underwent restructuring upon binding of the peptide substrate to the catalytic metal ion. Specifically, we detected an expected[33] relative increase in zinc coordination number during the kinetic lag phase (**Fig. 3**, black arrow), which indicated the formation of a pentacovalent complex at the catalytic zinc ion (**Table 1**). We used principal component analysis (PCA)[45] to identify the number of different intermediate species and their relative abundance. **Figure 2c** shows the relative population of the active pentacovalent intermediate during the catalytic cycle. The peptide substrate gradually populated the zinc ion during the kinetic lag phase, as a function of time. At 50 ms, only the enzymes were bound to the peptide substrate through the catalytic zinc ion, as indicated by XAS analysis (**Table 1, Fig. 2c**).

Our combined time-resolved analyses indicate that the net change in coupled protein-water motions, as observed by KITA (**Fig. 2b**), is correlated in time with the formation of the catalytically active Michaelis complex at the enzyme-catalytic zinc ion. Moreover, the dynamic changes in coordination number of the catalytic zinc ion were accompanied by shifts in the zinc K-edge energy of the raw XAS data, which are attributed to changes in the total effective charge of the zinc ion (**Fig. 2d**). These effective charge fluctuations were previously shown to be associated with partial reduction and a subsequent oxidation of the catalytic zinc ion during catalysis[33]. The dynamic polarization of the zinc ion during turnover was attributed to local structural reorganization of the enzyme catalytic site and partial charge transitions during the chemical reaction. Spectral transitions of these structural changes can be directly correlated with dynamic changes in coupled protein-water motions during the reaction lag phase.

Hydration dynamics correlate with Michaelis complex formation

As a control, we conducted time-resolved fluorescence and KITA studies following substrate hydrolysis using a ‘poor’ peptide substrate. This peptide substrate possesses a recognition sequence that is less preferred by MT1-MMP. This substrate is thus hydrolyzed

slower than the 6-mer substrate observed by steady state kinetics[46]. Time-resolved kinetic fluorescence analysis, which was conducted under conditions identical to those used for the 6-mer substrate, revealed a substantially extended kinetic lag phase of ~100 ms (**Fig. 4a**). Accordingly, KITA measurements yielded a net decrease in THz absorption before peptide hydrolysis, with a relaxation time of ~140 ms (**Fig. 4b**), which we found to be correlated in time with the kinetic lag phase of the enzymatic reaction in the presence of the 'poor' substrate. These results are consistent with the fluorescence and KITA spectral patterns observed for the 6-mer peptide substrate.

To prove that the observed time-dependent changes in THz absorption are correlated with enzyme turnover (peptide hydrolysis), we repeated the combined XAS-KITA real-time analyses using a specific protein inhibitor of MT1-MMP, tissue inhibitor of MMP2 (TIMP-2). TIMP-2 binds MT1-MMP with high affinity (nM range) by directly coordinating the catalytic zinc ion that is followed by displacement of water from the enzyme active site and binding interface[47,48]. We conducted time-dependent analysis of MT1-MMP and TIMP-2 complex formation by monitoring the change in the intrinsic tryptophan fluorescence of the enzyme. We observed an increase in tryptophan fluorescence during the first 400 ms (**Fig. 4c**), indicating complex formation between MT1-MMP and TIMP-2. Stopped-flow XAS analysis detected a pentacoordinated complex at the zinc ion upon binding of TIMP-2 after 200 ms (**Supplementary Table 1**). Binding of TIMP-2 to the catalytic zinc ion is consistent with X-ray crystallography studies[47,48].

Our KITA analysis of the interaction between MT1-MMP and TIMP-2 is shown in **Figure 4d**. The detected net change of 0.8% in THz absorption may be attributed to the displacement of water from the enzyme active site and protein binding interface in the absence of catalysis. The overall change in the net THz absorption was considerably smaller (that is, by a factor of 3) compared to the signal obtained during substrate turnover (**Fig. 2b**) and was only slightly above the noise level (**Fig. 4d**). These results further suggest that the 3% decrease in the KITA signal detected during the functional enzyme-substrate interaction cannot be attributed solely to pure water displacement upon substrate binding. Moreover, they show that the observed decay in KITA signal is correlated with structural changes and with associated fluctuations of the metal-ion effective charge measured during enzyme turnover (**Fig. 2**).

Gradient of protein-water motions around enzyme and substrate

Our combined time-resolved spectroscopic analyses indicated that changes in the coupled protein-water dynamics are intimately correlated with local atomic structural-kinetic transitions at the catalytic zinc ion of the enzyme active site. To gain further insights into the underlying molecular mechanism, we carried out molecular dynamics simulations (see **Supplementary Methods**). Molecular dynamics simulations can provide atomistic details on short- and long range coupled protein-water dynamics. In previous studies, we found that changes in the THz spectra of protein solutions are correlated with changes in the picosecond dynamics of the protein-water hydrogen bond network determined by molecular dynamics simulations[37,43]. Here, we studied the influence of enzyme-substrate interactions on the rearrangement dynamics of the protein-water hydrogen bond network. Specifically, we studied in detail hydration water dynamics around the substrate, the enzyme and the enzyme–substrate complex as well as local hydration water dynamics within the cleft at the catalytic site of MT1-MMP. In particular, we investigated the charge effect of the catalytic zinc ion on the solvent dynamics at the confined active site of the enzyme.

In order to correlate our experimental results with molecular dynamics simulations, we investigated two molecular scenarios that included (i) the free enzyme and the nonspecifically bound substrate and (ii) the productive Michaelis complex. We calculated

the average times for hydrogen bond rearrangements from the decay of the corresponding hydrogen bond time-correlation function. Although statistically converged results for this process were obtained on subnanosecond time scales, for each of the studied systems we analyzed hydrogen bond rearrangements in independent constant-energy trajectories. The starting configurations were sampled from 12-ns constant-temperature simulations to account for slower structural fluctuations in the protein. In addition, the nonspecifically bound substrate was represented by an ensemble of ten independent simulations, 12 ns each, with the substrate being initially bound to different and unspecific locations at the enzyme surface (**Supplementary Fig. 2**).

First, we calculated hydration water dynamics of the free enzyme and the substrate that is nonspecifically bound to the enzyme, corresponding to the experimental conditions at $t = 0$ ms (**Supplementary Fig. 2**)[33]. We then analyzed hydration water dynamics for the reactive Michaelis complex in which the substrate is coordinated to the catalytic zinc ion of the enzyme (**Supplementary Fig. 3**). For water molecules solvating the free enzyme and the free substrate, we found a pronounced retardation in hydrogen bond rearrangement dynamics compared to bulk water (average hydrogen bond lifetime of 2.6 ps versus 1.5 ps) due to interactions with the protein (**Fig. 5a**). Hydrogen bonds between water molecules in close proximity to the unoccupied catalytic site (~100 water molecules) are substantially more long-lived than water molecules solvating the surface of the enzyme (~10,000 water molecules) and the nonspecifically bound substrate (**Fig. 5a**). Specifically, hydrogen bonds between water molecules within 6 Å of the atoms of the confined catalytic site remained intact an average of five times longer than in bulk water (7.2 versus 1.5 ps) and about 2.5 times longer than hydrogen bonds within the hydration shell of the enzyme or in close proximity to the nonspecifically bound peptide (7.2 versus 2.6 ps) (**Fig. 5a**). An increased retardation of water molecules solvating the bound peptide substrate with an average hydrogen bond lifetime of 3.5 ps could also be observed upon formation of the Michaelis complex (**Fig. 5a**). This retardation was less pronounced than for water molecules solvating the enzyme catalytic cleft, but it involved many more water molecules than the ~100 water molecules residing within close proximity (6 Å) to the enzyme active site.

Experimentally, we also found substantial changes in the THz absorption to be correlated with charge fluctuations at the metal-loenzyme active site (**Fig. 2b,d**). Thus, we tested *in silico* whether the catalytic zinc ion influences the hydration dynamics at the enzyme active site by varying the effective charge of the zinc ion in the active site from $q = 2$ to $q = 0$. We kept the architecture of the active site fixed, so any confinement effect on the hydration dynamics should have remained unaffected. Our molecular dynamics simulations show a substantial change in the retardation of water molecules solvating the catalytic site within a 6–Å distance from the metal ion, induced by the net charge of the metal ion (**Supplementary Fig. 4**). We thus conclude that the intrinsic metal ion—hence the general charge or chemical polarization of the enzyme active site—has a substantial impact on the hydration dynamics of the water molecules in the vicinity of the metal ion during turnover.

We propose that the observed exponential decrease in the net THz absorption upon substrate binding is related to alteration of the water motion gradient becoming more moderate upon formation of the Michaelis complex. The effect on hydrogen bond dynamics observed in the simulation cannot account for the full scale of the experimentally observed absorption change. A direct comparison of the THz spectra computed from the molecular dynamics simulations to the experiments cannot be achieved in current simulations because of the lack of polarization terms[39–43]. It was recently demonstrated that dynamic polarization is required to model the THz absorption spectra of water, whose features are otherwise absent[39,43]. However, we note that the retardation of hydrogen bond rearrangements in the hydration water of proteins is typically accompanied by a blue shift of vibrational modes

centered at ~1.5 THz (**Supplementary Fig. 5**), which is accessible by the calculated vibrational density of states, even for nonpolarizable models[43]. This leads to a reduced mode density below the 1.5 THz frequency and to a corresponding increase at higher frequency (>1.5 THz) that resemble the experimentally observed changes in the THz absorption of hydration water[37,43].

In our molecular dynamics simulations, we used the retardation of hydration water dynamics as an indicator for variations in picosecond dynamics and corresponding changes in the THz absorption. When simulating an ensemble of unspecific enzyme-substrate complexes (resembling the molecular conditions during the kinetic lag phase of the experiment), we observed local changes in hydration water dynamics at the enzyme active site and around the peptide substrate. The retarded hydrogen bond dynamics provides the basis for understanding the experimentally observed pronounced 3% change in net THz absorption.

DISCUSSION

For a long time, the proposed link between water motions and protein dynamics during enzyme catalysis remained elusive because of a lack of effective experimental tools to study this phenomenon. Computational studies suggest that the correlation of the motions of protein and solvent could be involved in increasing the frequency of barrier crossing during turnover[49] or that energy transferred from first hydration shell of a protein to its surface residues could affect catalysis through network fluctuations[50]. Other studies[30] have recently used microspectrophotometry to simultaneously measure solvent dynamics and functional kinetics in flash-cooled enzyme solutions. These studies demonstrated that changes in water dynamics are associated with the formation of distinct reaction intermediates during oxidoreductase turnover.

By combining state-of-the-art, real-time structural spectroscopic tools, we have identified a molecular mechanism by which retardation of water dynamics is connected to the formation of the Michaelis complex during the enzymatic reaction studied here. Our results indicate a pronounced change in the gradient of hydration water dynamics at different stages of the enzyme reaction (**Fig. 5a,b**). Specifically, a steep gradient of water motions (slow to fast) is generated at the enzyme active site ranging from slow water molecules solvating the active site to faster, more bulk-like water molecules. Upon the formation of the Michaelis complex, the collective water dynamics is altered to form a moderate water motion gradient (**Fig. 5b**, right).

We here propose that the observed water motion gradient may assist substrate binding through a remote mechanism of water polarization and dynamics induced by (i) conformational transitions of the peptide substrate translocating over the enzyme surface, (ii) expected enzyme backbone dynamics and (iii) structural-kinetic transitions at the charged zinc ion residing at the active site (**Figs. 2** and **3**). Thus, coupled protein-water hydrogen bond network dynamics might play a role in enhancing local chemical or electrostatic protein conformational transitions that are important to enzyme function. Intrinsic slow hydrogen bond dynamics generated at the enzyme active site and at the peptide substrate during its translocation to the active site may assist the formation of productive Michaelis complex by attenuating protein conformational transitions of both enzyme and substrate at the millisecond time scale. We expect that further experiments focusing on the interaction of enzymes with protein substrates of various shapes and sizes will shed additional light on the interplay between protein functional motions and water dynamics.

METHODS

Methods and any associated references are available in the online version of the paper at http://www.nature.com/nsmb/.

Supplementary Material

Refer to Web version on PubMed Central for supplementary material.

Acknowledgments

We thank A. Frenkel (Yeshiva University), J. Bohon, M. Sullivan (beam line X3B at the National Synchrotron Light Source), I. Solomonov and Y. Udi (Weizmann Institute of Science) for help with X-ray absorption data collection, and we thank M. Krüger (Ruhr-University Bochum) for programming the THz data acquisition software. We thank G. Murphy (Cambridge Research Institute) for the plasmid encoding TIMP-2. We acknowledge financial support by the Ministry of Innovation, Science, Research and Technology of the German state of North Rhine-Westphalia and by the Ruhr-University Bochum and thank the Ressourcenverbund North Rhine-Westphalia for computer time. B.B. and M.He. were members of the Ruhr-University Research School funded by Germany's Excellence Initiative (DFG GSC 98/1). B.B. is grateful to the Feinberg Graduate School at the Weizmann Institute for a Dean of Faculty fellowship. M.He. was a fellow of the Studienstiftung des Deutschen Volkes. G.B.F. is supported by the Robert A. Welch Foundation. G.B.F. and I.S. are supported by a US National Institutes of Health grant (CA098799). I.S. is supported by the Israel Science Foundation, the Kimmelman Center at the Weizmann Institute and the Ambach family fund. M.Ha. is supported by the VW Stiftung.

ONLINE METHODS

Expression and purification of MT1-MMP

The catalytic domain of human MT1-MMP (residues 114–290) was cloned into the pET3a expression vector (Novagen, EMD Chemical Groups) with an N-terminal His tag and expressed in the *Escherichia coli* BL21 strain (GE Healthcare). Following expression, the enzyme accumulated in inclusion bodies. *E. coli* bacteria were harvested, washed, lysed and centrifuged to isolate the inclusion bodies. The inclusion bodies were suspended in 6 M urea, 50 mM Tris, pH 8.5, to solubilize the protein. The protein was purified on a Ni-NTA column, diluted to 50 $\mu g\ ml^{-1}$ with 6 M urea in 50 mM Tris buffer, with 150 mM β-mercaptoethanol at pH 8.5. Refolding was carried out by slow dialysis against a gradient of decreasing urea concentrations. Finally, the enzyme was purified by size exclusion on a gel filtration column, Superdex 75 ($2.6 \times 60\ cm^2$ (Amersham Pharmacia Biotech)).

Steady-state kinetics

The turnover numbers, K_{cat}, of the enzymatic reactions were determined at 25 °C by monitoring the increased fluorescence intensity upon degradation of the fluorogenic peptides Mca-PLGL(Dnp)AR and Mca-Arg-Pro-Lys-Pro-Ala-Nva-Trp-Met-Lys(Dnp)-NH_2. The fluorescence emitted at $\lambda_{em} = 400$ nm was monitored after excitation at $\lambda_{em} = 340$ nm as described by Neumann *et al.*[36]. The standard assay mixture contained 50 mM Tris buffer at pH 7.5, 100 mM NaCl, 5 mM $CaCl_2$ and 0.05% (v/v) Brij.

Transient fluorescence kinetic studies

To follow the initial catalytic events during a single catalytic cycle, we used a stopped-flow instrument (Applied Photophysics SX18). Kinetic assays were conducted at 25 °C in assay buffer without Brij, under multiple turnover conditions ([S] > [E]). The activity of MT1-MMP was initiated by rapid mixing of 1 μM MT1-MMP with 20 μM of fluorogenic substrate and was monitored following the fluorescence increase at $\lambda_{em} > 380$ nm. Under these conditions, the reaction rate is not diffusion limited.

Kinetic terahertz absorption spectroscopy

MT1-MMP activity was initiated by 1:6 mixing of enzyme and substrate solutions in assay buffer using a stopped-flow cell (Unisoku) of 50 μm z-cut quartz windows and a volume of 40 μL. The final concentrations after mixing were 20 μM MT1-MMP and 400 μM substrate solution, keeping the [E:S] ratio at 1:20. A terahertz time-domain spectrometer (THz TDS) was combined with a stopped-flow cell and operated in transmission mode[51,52]. THz pulses were recorded using electro-optic sampling. For each data point, thirty terahertz kinetic traces were averaged. Subsequently, the THz pulse transmitting the buffer (E_{buffer}: mixing of buffer and buffer) and the THz pulse transmitting the enzyme-substrate mixture (E_{mix}: mixing of enzyme and substrate, both dissolved in buffer) were recorded. THz data were evaluated according to a procedure published previously[34] (**Supplementary Fig. 1** and **Supplementary Methods**).

Freeze-quench sample preparation

MT1-MMP was concentrated by ultra-filtration in 20 ml Vivaspin units (10 kDa cut-off; Vivascience AG, Germany) to a final concentration of 400 μM. MT1-MMP and nonfluorogenic peptides were mixed at 1:4 ratio (enzyme:substrate) and freeze-quenched in liquid nitrogen. Freeze-quench was carried out in aluminum sample holders (10 × 5 × 0.5 mm^3) covered with Mylar tape, using the BioKine SFM-300 freeze-quench module (SFM-300; Bio-Logic-Science Instruments SA). Distinct time points for freezing were chosen to be within a single catalytic cycle (0–750 ms). In order to avoid thermal disorder, which could affect the X-ray absorption spectroscopy data, frozen samples were kept in liquid nitrogen at 77 K until the XAS measurements were conducted at the synchrotron.

X-ray absorption spectroscopy data collection and analysis

XAS data collection was done at the National Synchrotron Light Source (NSLS, Brookhaven National Laboratory, beamline X3B). The spectra were recorded at the zinc K-edge in the fluorescence geometry at low temperature (40 K). The beam energy was defined using a flat silicon monochromator crystal cut in a (111) orientation. The incident beam intensity I_0 was recorded using an ionization chamber. The fluorescence intensity was recorded using a 13-element germanium detector. To calibrate the beam energy, the transmission signal from a zinc foil was measured with a reference ion chamber simultaneously with fluorescence. Several scans (5–13) of each sample were collected and averaged. Data processing and analysis is explained in detail in the **Supplementary Methods**. The number of different species in the samples at all time steps and the mixing fractions within the various trapped complexes were determined by applying principal component analysis, multiple dataset fits and residual phase analysis as described in **Supplementary Methods**. The XAS fit parameters were iteratively varied and fixed to examine the stability of each fit. Specifically, the E_0 shifts were varied while the distances and Debye-Waller factors were guessed. Data were fitted up to 3.3 Å including the first, second and third coordination shells.

Analysis of MT1-MMP and TIMP interaction

The plasmid encoding TIMP-2 was a gift from the lab of G. Murphy and the protein was overexpressed as described previously[53]. Transient kinetic analysis of MT1-MMP and TIMP-2 complex formation was conducted by monitoring the change in the intrinsic tryptophan fluorescence of MT1-MMP at λ_{ex} = 295 nm and λ_{em} = 320 nm, under identical conditions to the substrate hydrolysis experiment, using 1 μM MT1-MMP and 20 μM TIMP-2. Reaction intermediates were freeze-quenched at representative time points and

probed by XAS. The XAS data were processed and fitted according to the procedure described in **Supplementary Methods** and summarized in **Supplementary Table 1**. In addition, KITA analysis was conducted under the same reaction conditions.

Molecular dynamics simulations

Simulations were carried out using the GROMACS package[54]. The GROMOS96 force field[55] was applied for the enzyme and substrate and the rigid simple point charge (SPC) force field for water. The simulated systems were prepared from the PDB entry 1BUV[47]. Equilibration runs were followed by 12-ns simulations of each system at constant temperature (NVT). Ten snapshots were taken every nanosecond from the last 10 ns of each simulation. The snapshots were used as starting points for microcanonical (NVE) simulations, which were used for data evaluation. These NVE simulations were extended to 60 ps length and coordinates and velocities were saved every 10 fs. The simulations were then used for the analysis of water dynamics in terms of water-water hydrogen bond autocorrelation functions $C_{HB}(t)$ and for the vibrational density of states (VDOS) of water oxygens (**Supplementary Methods**).

References

1. Koshland DE. Application of a theory of enzyme specificity to protein synthesis. Proc. Natl. Acad. Sci. USA. 1958; 44:98–104. [PubMed: 16590179]
2. Benkovic SJ, Hammes GG, Hammes-Schiffer S. Free-energy landscape of enzyme catalysis. Biochemistry. 2008; 47:3317–3321. [PubMed: 18298083]
3. Henzler-Wildman KA, et al. A hierarchy of timescales in protein dynamics is linked to enzyme catalysis. Nature. 2007; 450:913–916. [PubMed: 18026087]
4. Benkovic SJ, Hammes-Schiffer S. A perspective on enzyme catalysis. Science. 2003; 301:1196–1202. [PubMed: 12947189]
5. Bourgeois D, Royant A. Advances in kinetic protein crystallography. Curr. Opin. Struct. Biol. 2005; 15:538–547. [PubMed: 16129597]
6. Dodson GG, Lane DP, Verma CS. Molecular simulations of protein dynamics: new windows on mechanisms in biology. EMBO Rep. 2008; 9:144–150. [PubMed: 18246106]
7. Eisenmesser EZ, et al. Intrinsic dynamics of an enzyme underlies catalysis. Nature. 2005; 438:117–121. [PubMed: 16267559]
8. Mittermaier A, Kay LE. New tools provide new insights in NMR studies of protein dynamics. Science. 2006; 312:224–228. [PubMed: 16614210]
9. Pieper J, et al. Temperature- and hydration-dependent protein dynamics in photosystem II of green plants studied by quasielastic neutron scattering. Biochemistry. 2007; 46:11398–11409. [PubMed: 17867656]
10. Schotte F, et al. Watching a protein as it functions with 150-ps time-resolved X-ray crystallography. Science. 2003; 300:1944–1947. [PubMed: 12817148]
11. Zaccai G. How soft is a protein? A protein dynamics force constant measured by neutron scattering. Science. 2000; 288:1604–1607. [PubMed: 10834833]
12. Nashine VC, Hammes-Schiffer S, Benkovic SJ. Coupled motions in enzyme catalysis. Curr. Opin. Chem. Biol. 2010; 14:644–651. [PubMed: 20729130]
13. Kamerlin SC, Warshel A. At the dawn of the 21st century: Is dynamics the missing link for understanding enzyme catalysis? Proteins. 2010; 78:1339–1375. [PubMed: 20099310]
14. Schwartz SD, Schramm VL. Enzymatic transition states and dynamic motion in barrier crossing. Nat. Chem. Biol. 2009; 5:551–558. [PubMed: 19620996]
15. Marlow MS, Dogan J, Frederick KK, Valentine KG, Wand AJ. The role of conformational entropy in molecular recognition by calmodulin. Nat. Chem. Biol. 2010; 6:352–358. [PubMed: 20383153]

16. Barron LD, Hecht L, Wilson G. The lubricant of life: a proposal that solvent water promotes extremely fast conformational fluctuations in mobile heteropolypeptide structure. Biochemistry. 1997; 36:13143–13147. [PubMed: 9376374]
17. Fenimore PW, Frauenfelder H, McMahon BH, Young RD. Bulk-solvent and hydration-shell fluctuations, similar to alpha- and beta-fluctuations in glasses, control protein motions and functions. Proc. Natl. Acad. Sci. USA. 2004; 101:14408–14413. [PubMed: 15448207]
18. Frauenfelder H, Fenimore PW, Chen G, McMahon BH. Protein folding is slaved to solvent motions. Proc. Natl. Acad. Sci. USA. 2006; 103:15469–15472. [PubMed: 17030792]
19. Hunt NT, Kattner L, Shanks RP, Wynne K. The dynamics of water-protein interaction studied by ultrafast optical Kerr-effect spectroscopy. J. Am. Chem. Soc. 2007; 129:3168–3172. [PubMed: 17315992]
20. Dér A, et al. Interfacial water structure controls protein conformation. J. Phys. Chem. B. 2007; 111:5344–5350. [PubMed: 17458989]
21. Papoian GA, Ulander J, Eastwood MP, Luthey-Schulten Z, Wolynes PG. Water in protein structure prediction. Proc. Natl. Acad. Sci. USA. 2004; 101:3352–3357. [PubMed: 14988499]
22. Klibanov AM. Improving enzymes by using them in organic solvents. Nature. 2001; 409:241–246. [PubMed: 11196652]
23. Levitt M, Park BH. Water: now you see it, now you don't. Structure. 1993; 1:223–226. [PubMed: 8081736]
24. Levy Y, Onuchic JN. Water mediation in protein folding and molecular recognition. Annu. Rev. Biophys. Biomol. Struct. 2006; 35:389–415. [PubMed: 16689642]
25. Cheung MS, Garcia AE, Onuchic JN. Protein folding mediated by solvation: water expulsion and formation of the hydrophobic core occur after the structural collapse. Proc. Natl. Acad. Sci. USA. 2002; 99:685–690. [PubMed: 11805324]
26. Rhee YM, Sorin EJ, Jayachandran G, Lindahl E, Pande VS. Simulations of the role of water in the protein-folding mechanism. Proc. Natl. Acad. Sci. USA. 2004; 101:6456–6461. [PubMed: 15090647]
27. Chaplin M. Do we underestimate the importance of water in cell biology? Nat. Rev. Mol. Cell Biol. 2006; 7:861–866. [PubMed: 16955076]
28. Eisenmesser EZ, Bosco DA, Akke M, Kern D. Enzyme dynamics during catalysis. Science. 2002; 295:1520–1523. [PubMed: 11859194]
29. Robinson CR, Sligar SG. Changes in solvation during DNA binding and cleavage are critical to altered specificity of the EcoRI endonuclease. Proc. Natl. Acad. Sci. USA. 1998; 95:2186–2191. [PubMed: 9482860]
30. Durin G, et al. Simultaneous measurements of solvent dynamics and functional kinetics in a light-activated enzyme. Biophys. J. 2009; 96:1902–1910. [PubMed: 19254549]
31. Daniel RM, Dunn RV, Finney JL, Smith JC. The role of dynamics in enzyme activity. Annu. Rev. Biophys. Biomol. Struct. 2003; 32:69–92. [PubMed: 12471064]
32. Kleifeld O, Frenkel A, Martin JM, Sagi I. Active site electronic structure and dynamics during metalloenzyme catalysis. Nat. Struct. Biol. 2003; 10:98–103. [PubMed: 12524531]
33. Solomon A, Akabayov B, Frenkel A, Milla ME, Sagi I. Key feature of the catalytic cycle of TNF-alpha converting enzyme involves communication between distal protein sites and the enzyme catalytic core. Proc. Natl. Acad. Sci. USA. 2007; 104:4931–4936. [PubMed: 17360351]
34. Kim SJ, Born B, Havenith M, Gruebele M. Real-time detection of protein-water dynamics upon protein folding by terahertz absorption spectroscopy. Angew. Chem. Int. Edn Engl. 2008; 47:6486–6489.
35. Osenkowski P, Toth M, Fridman R. Processing, shedding, and endocytosis of membrane type 1-matrix metalloproteinase (MT1-MMP). J. Cell. Physiol. 2004; 200:2–10. [PubMed: 15137052]
36. Neumann U, Kubota H, Frei K, Ganu V, Leppert D. Characterization of Mca-Lys-Pro-Leu-Gly-Leu-Dpa-Ala-Arg-NH2, a fluorogenic substrate with increased specificity constants for collagenases and tumor necrosis factor converting enzyme. Anal. Biochem. 2004; 328:166–173. [PubMed: 15113693]
37. Ebbinghaus S, et al. An extended dynamical hydration shell around proteins. Proc. Natl. Acad. Sci. USA. 2007; 104:20749–20752. [PubMed: 18093918]

38. Heugen U, et al. Solute-induced retardation of water dynamics probed directly by terahertz spectroscopy. Proc. Natl. Acad. Sci. USA. 2006; 103:12301–12306. [PubMed: 16895986]
39. Heyden M, et al. Dissecting the THz spectrum of liquid water from first principles through correlations in time and space. Proc. Natl. Acad. Sci. USA. 2010; 107:12068–12073. [PubMed: 20566886]
40. Pal SK, Peon J, Zewail AH. Biological water at the protein surface: dynamical solvation probed directly with femtosecond resolution. Proc. Natl. Acad. Sci. USA. 2002; 99:1763–1768. [PubMed: 11842218]
41. Fenimore PW, Frauenfelder H, McMahon BH, Parak FG. Slaving: solvent fluctuations dominate protein dynamics and functions. Proc. Natl. Acad. Sci. USA. 2002; 99:16047–16051. [PubMed: 12444262]
42. Arikawa T, Nagai M, Tanaka K. Characterizing hydration state in solution using terahertz time-domain attenuated total reflection spectroscopy. Chem. Phys. Lett. 2008; 457:12–17.
43. Heyden M, Havenith M. Combining THz spectroscopy and MD simulations to study protein-hydration coupling. Methods. 2010; 52:74–83. [PubMed: 20685393]
44. Rosenblum G, et al. Molecular structures and dynamics of the stepwise activation mechanism of a matrix metalloproteinase zymogen: challenging the cysteine switch dogma. J. Am. Chem. Soc. 2007; 129:13566–13574. [PubMed: 17929919]
45. Frenkel AI, Kleifeld O, Wasserman SR, Sagi I. Phase speciation by extended X-ray absorption fine structure spectroscopy. J. Chem. Phys. 2002; 116:9449–9456.
46. Nagase H, Fields CG, Fields GB. Design and characterization of a fluorogenic substrate selectively hydrolyzed by stromelysin 1 (matrix metalloproteinase-3). J. Biol. Chem. 1994; 269:20952–20957. [PubMed: 8063713]
47. Fernandez-Catalan C, et al. Crystal structure of the complex formed by the membrane type 1-matrix metalloproteinase with the tissue inhibitor of metalloproteinases-2, the soluble progelatinase A receptor. EMBO J. 1998; 17:5238–5248. [PubMed: 9724659]
48. Grossman M, et al. The intrinsic protein flexibility of endogenous protease inhibitor TIMP-1 controls its binding interface and affects its function. Biochemistry. 2010; 49:6184–6192. [PubMed: 20545310]
49. Bruice TC, Benkovic SJ. Chemical basis for enzyme catalysis. Biochemistry. 2000; 39:6267–6274. [PubMed: 10828939]
50. Agarwal PK. Role of protein dynamics in reaction rate enhancement by enzymes. J. Am. Chem. Soc. 2005; 127:15248–15256. [PubMed: 16248667]
51. Exter, M.v.; Fattinger, C.; Grischkowsky, D. Terahertz time-domain spectroscopy of water vapor. Opt. Lett. 1989; 14:1128–1130. [PubMed: 19753077]
52. Kindt JT, Schmuttenmaer CA. Far-infrared dielectric properties of polar liquids probed by femtosecond terahertz pulse spectroscopy. J. Phys. Chem. 1996; 100:10373–10379.
53. Lee MH, Rapti M, Knauper V, Murphy G. Threonine 98, the pivotal residue of tissue inhibitor of metalloproteinases (TIMP)-1 in metalloproteinase recognition. J. Biol. Chem. 2004; 279:17562–17569. [PubMed: 14734567]
54. Spoel DVD, et al. GROMACS: Fast, flexible, and free. J. Comput. Chem. 2005; 26:1701–1718. [PubMed: 16211538]
55. Scott WRP, et al. The GROMOS biomolecular simulation program package. J. Phys. Chem. A. 1999; 103:3596–3607.

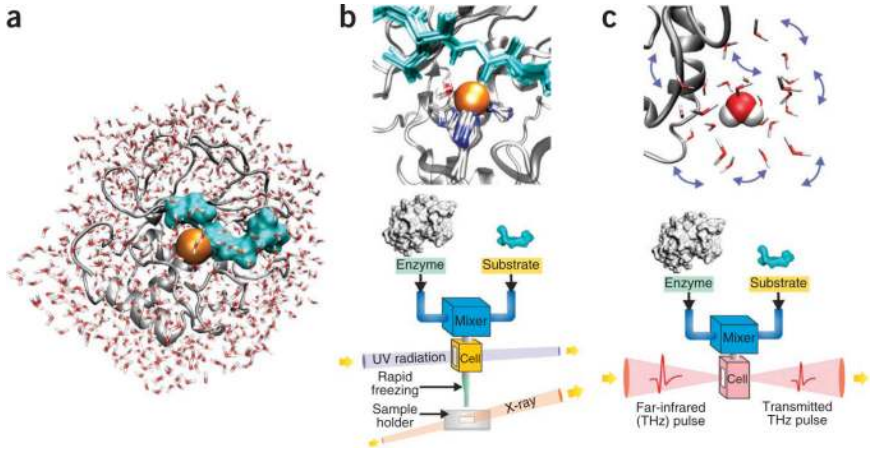

Figure 1.

Schematic illustration of the experimental setup to measure structural kinetics and solvation dynamics of metalloenzymes in real time. (**a**) Human MT1-MMP (gray, catalytic domain, residues 114–291) surrounded by water molecules (sticks) and bound to a peptide substrate (cyan). The catalytic zinc ion is shown as a sphere (orange). (**b**) In the enzyme active site, the zinc ion is coordinated to three histidine residues (in sticks) and to a water molecule. The active site structural kinetics are probed by transient kinetic analysis of the hydrolysis of a fluorogenic peptide using a stopped-flow device. The enzyme and the peptide substrate are rapidly mixed and the change in fluorescence intensity is detected with milliseconds time resolution. At representative times, the solution is rapidly freeze-quenched and probed by XAS at the zinc K-edge energy, providing the metal ion oxidation state, coordination number, bond distances and disorder. (**c**) Changes in the collective water network dynamics of the enzyme-substrate mixture during enzymatic turnover are probed by THz pulses in the KITA experiment. At selected times after mixing, the net THz absorption is recorded.

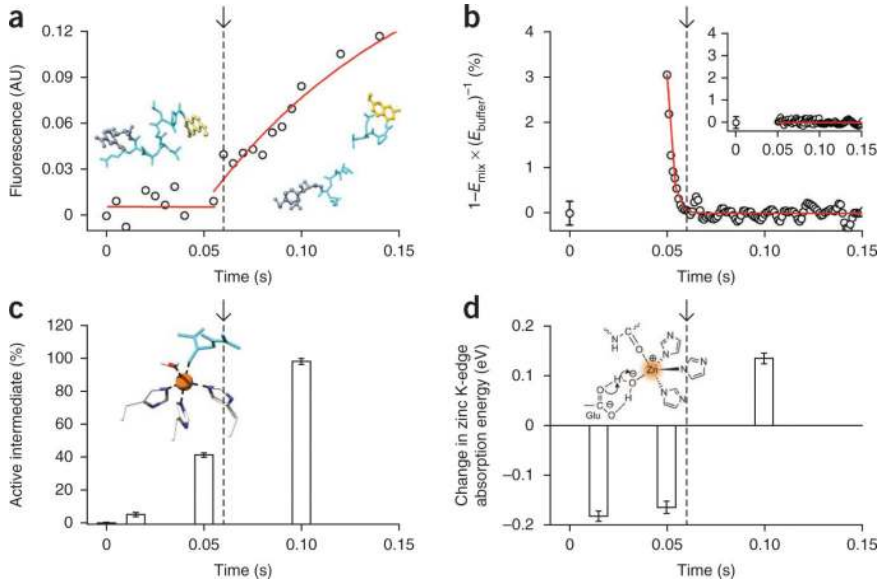

Figure 2.

Real-time spectroscopic analysis of metalloenzyme (MT1-MMP) catalysis of the peptide substrate Mca-PLGL(Dnp)AR. (**a**) Pre-steady state analysis showing the fluorescence emission (○) after mixing MT1-MMP and the fluorogenic substrate Mca-PLGL(Dnp)AR in a stopped-flow apparatus ($\lambda_{excitation}$ (λ_{ex}) = 340 nm, $\lambda_{emission}$ (λ_{em}) > 380 nm). Fluorescence intensity is displayed in arbitrary units (AU). A 60 ms kinetic lag phase precedes a kinetic burst (dashed line and arrow). Inset, intact substrate (left) and products of substrate hydrolysis (right). (**b**) KITA (○) showing the time-resolved transmitted electric field amplitude of the THz pulse for the enzyme-substrate mixture (E_{mix}) as well as for the buffer (E_{buffer}) under experimental conditions identical to those for **a**. Inset, KITA of buffer-buffer mixing. (**c**) Increased formation of the active intermediate, correlated with changes in solvent dynamics. The relative fractions of the pentacovalent active intermediate (in columns) were determined by principal component analysis on XAS analysis of the MT1-MMP catalytic site during substrate turnover. Error bars are from the residuals of the principal component analysis. Inset, structure of the pentacoordinated Michaelis complex. (**d**) Active site charge fluctuations during substrate binding and turnover (in columns) derived from the shifts in zinc K-edge absorption energies ± s.e.m. Inset, representative charge fluctuations at the catalytic zinc ion of MT1-MMP during turnover.

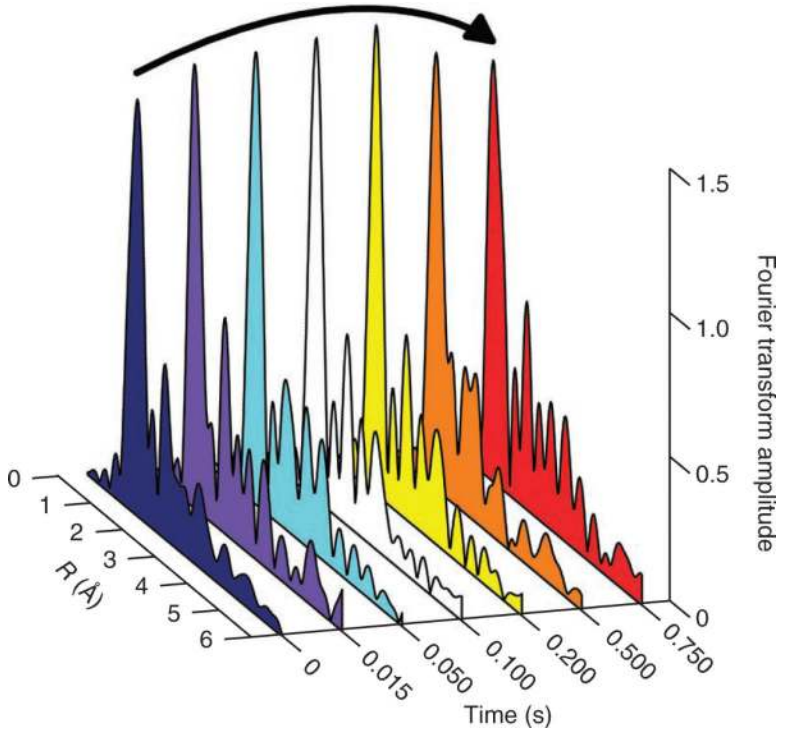

Figure 3.

Analysis of time-dependent X-ray absorption spectra. The data are presented in the form of Fourier transform spectra to provide the radial distribution of the atoms within the first and second coordination shell of the catalytic zinc ion in MT1-MMP, where *R* is the zinc-ligand bond distance in angstroms (Å). The shape and amplitude of the Fourier transform peaks are directly related to the type and number of amino acid residues that are bound to the zinc ion. The increase in the first shell amplitude is correlated with an increase in coordination number (curved black arrow).

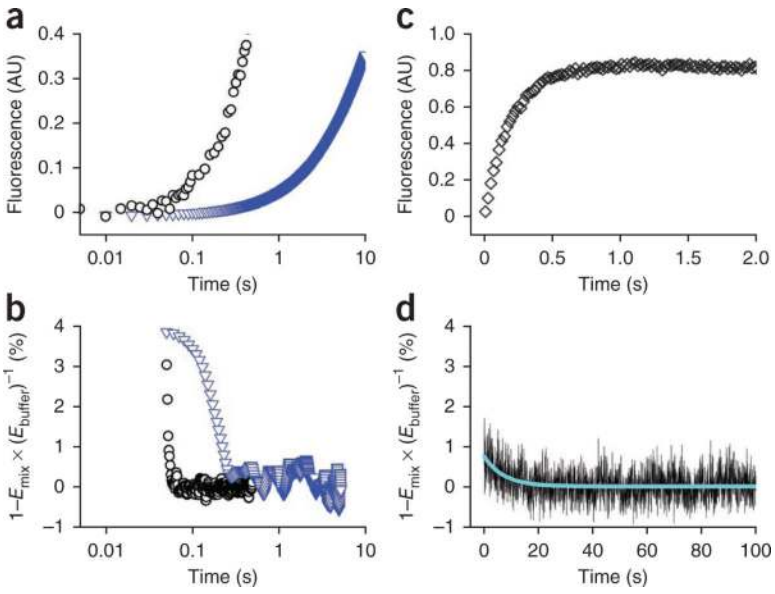

Figure 4.

Changes in hydration dynamics are mostly associated with Michaelis complex formation. (**a**) Comparison between the transient kinetic traces of hydrolysis of 6-mer peptide substrate (○) versus a 'poor' substrate (blue triangles) of the sequence Mca-Arg-Pro-Lys-Pro-Ala-Nva-Trp-Met-Lys(Dnp)-NH_2 (Nva = norvaline) by MT1-MMP. The kinetic analysis (shown in log scale for clarity) features an extended lag phase of 100 ms. (**b**) An extended exponential decay in net THz absorption of 140 ms is observed during hydrolysis of the 'poor' peptide substrate by MT1-MMP, synchronized with the kinetic lag phase (blue triangles). (**c**) The interaction between MT1-MMP and its endogenous inhibitor TIMP-2 was monitored by the increase in the MT1-MMP intrinsic fluorescence (◇). Complex formation is achieved within 400 ms. (**d**) The change in solvent dynamics during MT1-MMP–TIMP-2 interaction probed by KITA is not found to be synchronized with complex formation. The time constant, when assuming an exponential decrease, is on the order of 7 s. The net change of THz absorption is on the order of 0.8%. AU, arbitrary units.

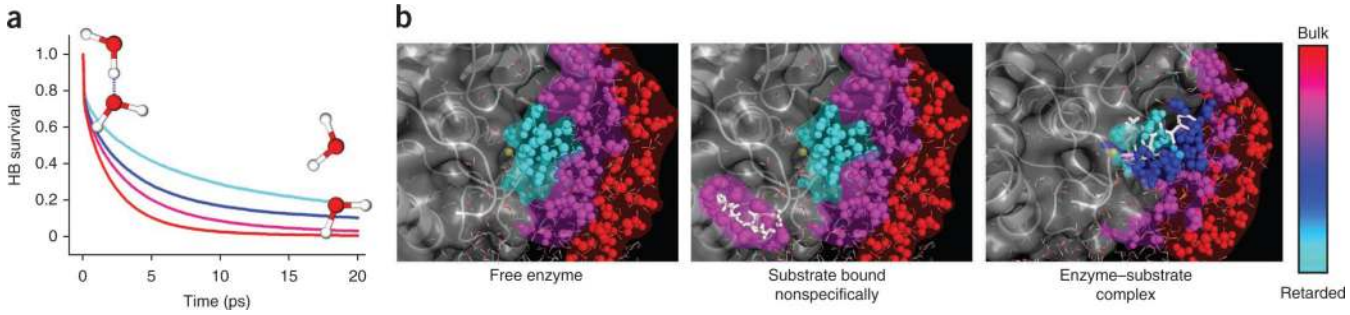

Figure 5.

Gradient of coupled protein-water motions. (**a**) Changes in hydration dynamics upon Michaelis complex formation. Shown are the averaged hydrogen bond lifetimes τ_{HB} of bulk water (red line; distance to closest protein atom >12 Å), water molecules solvating MT1-MMP (magenta line; distance to closest enzyme atom <6 Å), water molecules solvating the bound substrate (blue line; distance to closest substrate atom <6 Å), and water molecules solvating the zinc ion of the free catalytic site before substrate binding (cyan line; distance to zinc ion <6 Å). (**b**) Water dynamics gradient at catalytic site and response upon complex formation. Selected water molecules from each hydration water layer are presented as spheres for clarity and are color coded as in **a**. The enzyme surface is shown in gray and the catalytic zinc ion as a yellow sphere. Left: a steep gradient of water motions (from strongly retarded water molecules (blue) to bulk (red)) is detected in the free enzyme before substrate binding to the catalytic zinc ion. Middle: initially, substrate molecules (white) nonspecifically bind to the enzyme surface. Hydration water molecules of the substrate show dynamics similar to enzyme hydration water. The overall gradient in the hydrogen bond dynamics at the active site is proposed to assist peptide binding through a remote water-retardation mechanism mediated by the charged metalloenzyme active site. Right: after substrate binding to the zinc ion, a smooth gradient of water hydrogen bond dynamics motions is generated while the water molecules solvating the substrate are slowed down (blue).

Table 1

X-ray absorption spectroscopy nonlinear fitting analysis of zinc-protein–ligand intermediates

Time (ms)	ΔE_0 (eV)	N	R (Å)	σ^2 (Å^2)
0	1.3 ± 0.4	4	1.99 ± 0.01	$1.9 \times 10^{-3} \pm 6.6 \times 10^{-4}$
15	6.2 ± 1.1	4	2.00 ± 0.01	$9.1 \times 10^{-4} \pm 1.1 \times 10^{-3}$
		1	2.23 ± 0.02	$8.9 \times 10^{-3} \pm 4.6 \times 10^{-3}$
50	3.2 ± 0.5	5	2.00 ± 0.01	$3.0 \times 10^{-3} \pm 1.2 \times 10^{-3}$
100	2.2 ± 0.6	5	1.99 ± 0.01	$3.0 \times 10^{-3} \pm 1.0 \times 10^{-3}$
200	2.6 ± 0.8	5	1.99 ± 0.01	$2.3 \times 10^{-4} \pm 1.2 \times 10^{-3}$

The raw X-ray absorption spectra during a single catalytic cycle of MT1-MMP were processed and analyzed following reported procedures[33] (**Supplementary Methods**). Presented are the best-fit parameters of the first coordination shell of the residual spectra resulting from iterative subtractions of fractions of the starting phases ($t = 0$), where N is the coordination number, R is the zinc-ligand bond distance in angstroms and σ^2 is the Debye-Waller factor. The pentacoordiated intermediate is detected at 15–200 ms.